INTERNATIONAL JOURNAL OF CLIMATOLOGY
Int. J. Climatol. (in press)
Published online in Wiley InterScience
(www.interscience.wiley.com) DOI: 10.1002/joc.1490

Intercomparison of global cloud cover fields over oceans from the VOS observations and NCEP/NCAR reanalysis

Ernst Bedacht,[a] Sergey K. Gulev[b] and Andreas Macke[a],*
[a] *Leibniz Institute of Marine Sciences, IFM-GEOMAR, Kiel, Germany*
[b] *P. P. Shirshov Institute of Oceanology, RAS, Moscow, Russia*

Abstract:

The paper inter-compares the total cloud cover over the World Ocean from marine visual observations assimilated in the International Comprehensive Ocean-Atmosphere Data Set (ICOADS) and National Centers of Environmental Prediction/National Center of Atmospheric Research (NCEP-NCAR) reanalysis. The Intercomparison covers the period from 1948 to 2002. NCEP-NCAR reanalysis shows about 10% of fractional cloud cover smaller than the visual observations do. The largest differences are observed in the mid and sub-polar latitudes. In the tropics, NCEP-NCAR data show slightly higher cloud cover then ICOADS. These systematic differences are quite persistent through the year with somewhat stronger differences in summer. Comparison of the characteristics of inter-annual variability shows little consistency between visually observed total cloud cover and total cloudiness diagnosed by the reanalysis. Linear trends are primarily positive in the ICOADS cloud data, while in the NCEP-NCAR reanalysis they show downward trends in the tropics and upward tendencies in the mid and high latitudes. Analysis of the effect of sampling in ICOADS shows that sampling inhomogeneity cannot fully explain the disagreements observed. At the same time, the major climate variability patterns such as North Atlantic Oscillation (NAO) and El-Nino – Southern Oscillation (ENSO) are well captured in both ICOADS and NCEP-NCAR cloud cover data sets. Copyright © 2007 Royal Meteorological Society

KEY WORDS clouds; ICOADS; NCEP-NCAR; climatology; NAO; ENSO; reanalysis

Received 9 August 2006; Accepted 1 December 2006

INTRODUCTION

Being formed by the condensation and sublimation of water vapour, cloudiness has signatures of all types of atmospheric motions (Rossow, 1978). Clouds play the most important role in forming the Earth radiation budget. Since the cloud albedo effect is larger than its greenhouse effect, clouds are typically cooling the climate system (Poetzsch-Heffter *et al*., 1995; Wielicki *et al*., 1995). However, different cloud types may affect the radiation budget to a different extent. According to Chen *et al*. (2000), the global mean net flux for cirrus is $+19.6$ W/m^2, whereas cumulus are cooling with -27.8 W/m^2. Clouds are involved in the freshwater and latent heat air–sea exchanges and the moisture transport between the oceans and the continents (e.g. Fowler and Randall, 1994; Wielicki *et al*., 1995). In this sense, the role of marine cloudiness is particularly important. Given the role of the World Ocean in the global energy balance (e.g. WGASF, 2000), marine cloudiness is a key parameter for the estimation of the short wave (SW) and long wave (LW) radiation at sea. Thus, accurate knowledge of the climate means and variability of marine cloudiness is very important for many budget and climate variability studies. At the same time, changes in even total cloud amounts are uncertain both over the subtropical and tropical land areas as well as over the oceans (IPCC, 2001).

Long-term global cloud data over the global ocean are presently available from satellite missions, such as the International Satellite Cloud Climatology Project ((ISCCP), Rossow and Schiffer, 1991; Rossow and Cairns, 1995; Rossow *et al*., 1996), from the long-term simulations with the operational atmospheric models in a data assimilation mode (the so-called reanalyses) and from observations of the Voluntary Observing Ships (VOS). Satellite cloud products are quite reliable over most ocean and land areas. The accuracy of quantification of the cloud cover from satellites depends on the radiance threshold that distinguishes between clear and cloudy pixels. The maximum limitations occur above snow- and ice-covered surfaces. The present ISCCP climatology is progressively improving and covers currently the period from July 1983 onwards. These data, however, do not exist for the decades prior to the mid 1980s and, thus, cannot be used for studies of climate variability on a multidecadal scale.

VOS cloud data represent visual reports of marine officers. Although observational accuracy of these data is not high, they are quite homogeneous in time, because

* Correspondence to: Andreas Macke, Leibniz-Institut für Meereswissenschaften, Ocean Circulation and Climate Dynamics, Düsternbrooker Weg 20, D-24105 Kiel, Germany. E-mail: amacke@ifm-geomar.de

the observational practice has not been changed since 1949. Cloud reports from VOS are assimilated in the International Comprehensive Ocean–Atmosphere Data Set (ICOADS) (Worley *et al.*, 2005), covering now the period from 1784 onwards. Warren *et al.* (1986) analysed visual observations of clouds over the land and later a similar analysis was performed by Warren *et al.* (1988) over the oceans using COADS data. Hahn *et al.* (1995) analysed different sources of uncertainties in the VOS cloud cover and particularly found the night observations to be less reliable than those obtained during daytime. Further comprehensive inventory of the marine cloud information from VOS (Hahn and Warren, 1999) documented most of the problems related to the accuracy of these observations. A specific problem of the VOS cloud data is spatial and temporal inhomogeneity of sampling. Although midlatitudinal regions of the Northern Hemisphere are primarily adequately sampled, in many areas of the Southern Ocean there are just a few cloud reports over several decades. Norris (1999) mentioned the potential possibility of artificial trends in marine cloud cover from VOS data due to regional changes of the number of reports and rerouting of the major ship tracks. Recently, Gulev *et al.* (2007a) presented estimates of sampling errors in most air–sea flux-related variables and fluxes and found that in poorly sampled regions sampling errors may be as important as observational errors. Nevertheless, VOS cloud data along with the other meteorological information from VOS form the basis for the long-term climatology of radiative fluxes over the ocean, computed using the so-called bulk-parameterizations (e.g. Reed, 1977; Dobson and Smith, 1988; Josey *et al.*, 1999; Fitzpatrick *et al.*, 2005), which were designed for visually observed cloud cover, available from VOS.

The reanalyses data (e.g. Kalnay *et al.*, 1996; Kistler *et al.*, 2001; Uppala *et al.*, 2006) cover periods of several decades, starting from the 1950s (ERA-40) and the late 1940s (NCEP-NCAR). Clouds in reanalyses are generated by the large-scale ascent, convection, boundary layer turbulence and radiative cooling, which all are parameterized in the atmospheric models used. As the other reanalysed variables, clouds are influenced by the changes in data assimilation input, especially for the period of the satellite epoch after the late 1980s. Evaluation of cloud cover from different reanalyses (Jacob, 1999; Trishchenko and Li, 2000; Kanamitsu *et al.*, 2002) shows that reanalysis clouds capture major spatial features of global distribution of clouds in the mid latitudes, however, show strong biases in the tropics. Global cloud cover from reanalyses is typically biased with respect to that observed from satellites by 10–15%. Given the growing interest of the climate community to the reanalyses, it is very timely now to compare means and variability patterns of cloud cover diagnosed by reanalyses with those based on the VOS cloudiness. Pilot validation of the Numerical Weather Prediction (NWP) cloud cover against nephanalyses clearly showed locally large differences, especially in the subtropics, where NWP systems produce too few low level stratus clouds (WGASF, 2000).

In this work, we perform an Intercomparison of the climatology and dominant modes of variability of the total cloud cover derived from the VOS data and NCEP/NCAR reanalysis. In our work, we tried to account for the two most important sources of potential disagreements between the two products – the quality of the cloud representation in the reanalyses and the spatial and temporal inhomogeneity of sampling in the VOS data. For this purpose, we simulated the VOS sampling in 6-h reanalyses data and quantified sampling-related uncertainties and the biases not associated with the VOS sampling by comparing with each other, the original and VOS-like sampled reanalysis cloud products on one hand and the VOS-based cloud climatology on the other. Section 2 describes the data sources and pre-processing. Section 3 compares global cloud climatology from the VOS and NCEP/NCAR for the period from 1948 to 2002. General characteristics of comparability of inter-annual variability in VOS and NCEP-NCAR cloud cover are presented in Section 4. Section 5 is focussed on the cloud signatures of the two climate phenomena – North Atlantic Oscillation (NAO) and El-Nino – Southern Oscillation (ENSO). In the 'Summary and Conclusions' section we summarize the inter-comparison.

DATA AND PRE-PROCESSING

In this study, we used visual estimates of the total cloud cover from the ICOADS for the period from 1948 to 2002 (Worley *et al.*, 2005). Cloudiness in ICOADS is given in octa categories. The code figure '09' stands for the obscure or not observed cloud cover. In order to produce a long-term gridded cloud cover product, we extracted the VOS reports including all cloud parameters. The number of reports containing only the total cloud cover is typically 10–20% higher than those reporting the whole set of cloud variables. We assumed that the reports with all cloud parameters were taken by better-trained officers and should have a higher observational accuracy. Thus, our product differs from that known as ICOADS Monthly Summary Trimmed Groups (MSTGs), developed by the ICOADS community (Woodruff *et al.*, 1998). In this study, we did not apply the correction for the moonlight recommended by Hahn *et al.* (1995), so that out estimates will be potentially biased by about 1–3% of cloud cover. Reports coded with figure '09' were not included in our pre-processing. Generally these reports should also increase the total cloud cover, as they typically represent the overcast conditions. The extracted reports were averaged for every calendar month and every 2-degree box over the World Ocean from 80 °S to 80°N for the period from 1948 to 2002.

Figure 1 shows the spatial distribution of the number of observations per 2-degree box per calendar month in selected VOS data and implies large spatial inhomogeneity of sampling affecting the cloud climatology. In the

DOI: 10.1002/joc

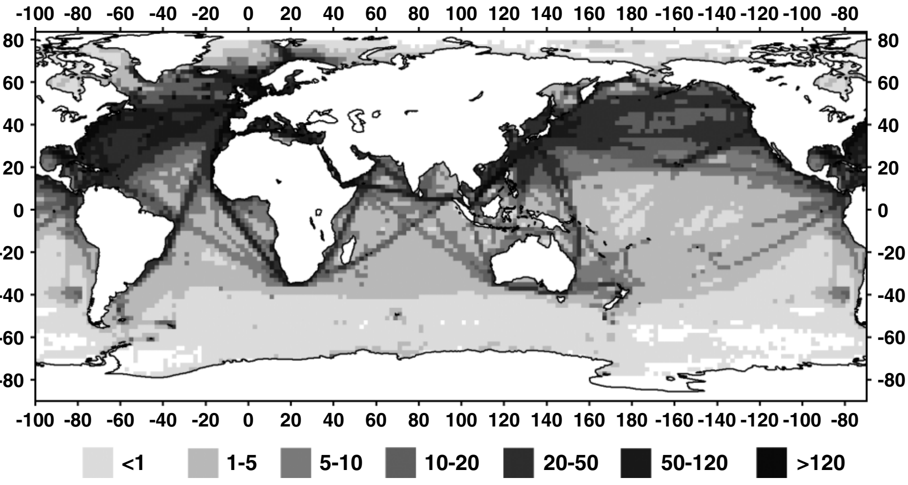

Figure 1. The total number of ICOADS cloud reports per calendar month per 2-degree box over the World Ocean over the period 1948–2002.

mid latitudes of the Northern Hemisphere, the number of reports per box per calendar months is typically higher than 20 and may match and over-predict the limit of 120, which represents the virtual 'sampling' provided by the 6-h reanalysis product for a 30-day month. However, in the Southern Hemisphere and in the areas out of major ship routes in the tropics and sub-polar latitudes of the Northern Hemisphere the number of reports may vary from 0 to 10, implying a strong potential impact of under-sampling on climatological cloud properties. The total number of cloud reports increased about 3–4 times from 1948 to the mid 1960s. Then it remained stable until the mid 1980s and decreased by about two times after that (Worley *et al*., 2005; Gulev *et al*., 2007a). Monthly averaging for 2-degree boxes was performed using 3.5 sigma trimming range, which is reasonable for the cloud cover, which is a finite parameter in contrast to say, temperatures. Given the generally wide range of synoptic intramonthly variability of cloud cover in most ocean areas, this limit has implied the observations to be outliers in just a few cases, primarily in the Mediterranean Sea in summer. Besides poorly sampled areas, there are 2-degree boxes, which do not have observations for some calendar months, especially in the Southern Hemisphere. The number of these boxes varies from 10% in the 1950s to a few per cent in the 1960s and 1970s. In order to produce the regular fields we used the modified method of local procedures (Akima, 1970) along with spatial smoothing with 2-dimensional Lancoz filtering (Duchon, 1979). These are exactly the algorithms used by Gulev *et al*. (2003, 2007a,b) for the other marine meteorological variables and fluxes. This is a common procedure for the development of global climatologies of the VOS individual variables and fluxes. Da Silva *et al*. (1994) and Josey *et al*. (1999) used somewhat different algorithms and one can find their pilot comparisons in Kent *et al*. (2000) and Gulev *et al*. (2007a). For the comparability with reanalysis cloud cover, the VOS cloud cover originally reported in the octa categories was recomputed into percentages.

Cloud cover from NCEP-NCAR reanalysis (Kalnay *et al*., 1996; Kistler *et al*., 2001), which covers the period from 1948 to 2002 with spatial resolution 1.875° by 1.92° and 6-hourly temporal resolution. From these data monthly mean fields were derived. In order to achieve comparability with the VOS data, NCEP-NCAR cloud fields were interpolated onto a 2-degree grid using the Akima (1970) local procedures method. In contrast to the VOS data, NCEP/NCAR fields are assumed to have a homogeneous sampling, i.e. each monthly mean is based on 112–124 6-h snapshots. The NCEP-NCAR 6-h cloud cover was also used in our study to generate the VOS-like sampled reanalysis data set. For this purpose, we used the methodology earlier suggested by Gulev *et al*. (2003, 2007). In order to simulate the VOS-like sampling, 6-h cloud data from reanalysis were matched to the dates and UTC hours of the ICOADS reports. If the ICOADS reports were not available at 'standard' times (00, 06, 12, 18), the adjacent snapshots were interpolated to the exact time of the VOS sample. In cases where more than one ICOADS report was available at one instant, the NWP fluxes were repeatedly used to simulate the oversampling of the VOS data. After the procedure of subsampling, the VOS-like sampled reanalysis cloud cover data were treated in the same manner as ICOADS reports, i.e. were averaged for 2-degree boxes and calendar months according to the guidelines described above. Thus, we obtained two NWP cloud cover products for the further comparisons – one based on the original regularly sampled NCEP-NCAR data and the other one, which was subsampled according to the actual ICOADS data coverage. Their further comparison with ICAODS gridded product will help to quantify differences associated with sampling and originating form the other than sampling reasons.

COMPARISON OF CLIMATOLOGICAL AND SEASONAL MEAN TOTAL CLOUD COVER FROM VOS AND NCEP-NCAR REANALYSIS

We start with the analysis of the long-term climatological mean total cloud cover in the two data sets for the

DOI: 10.1002/joc

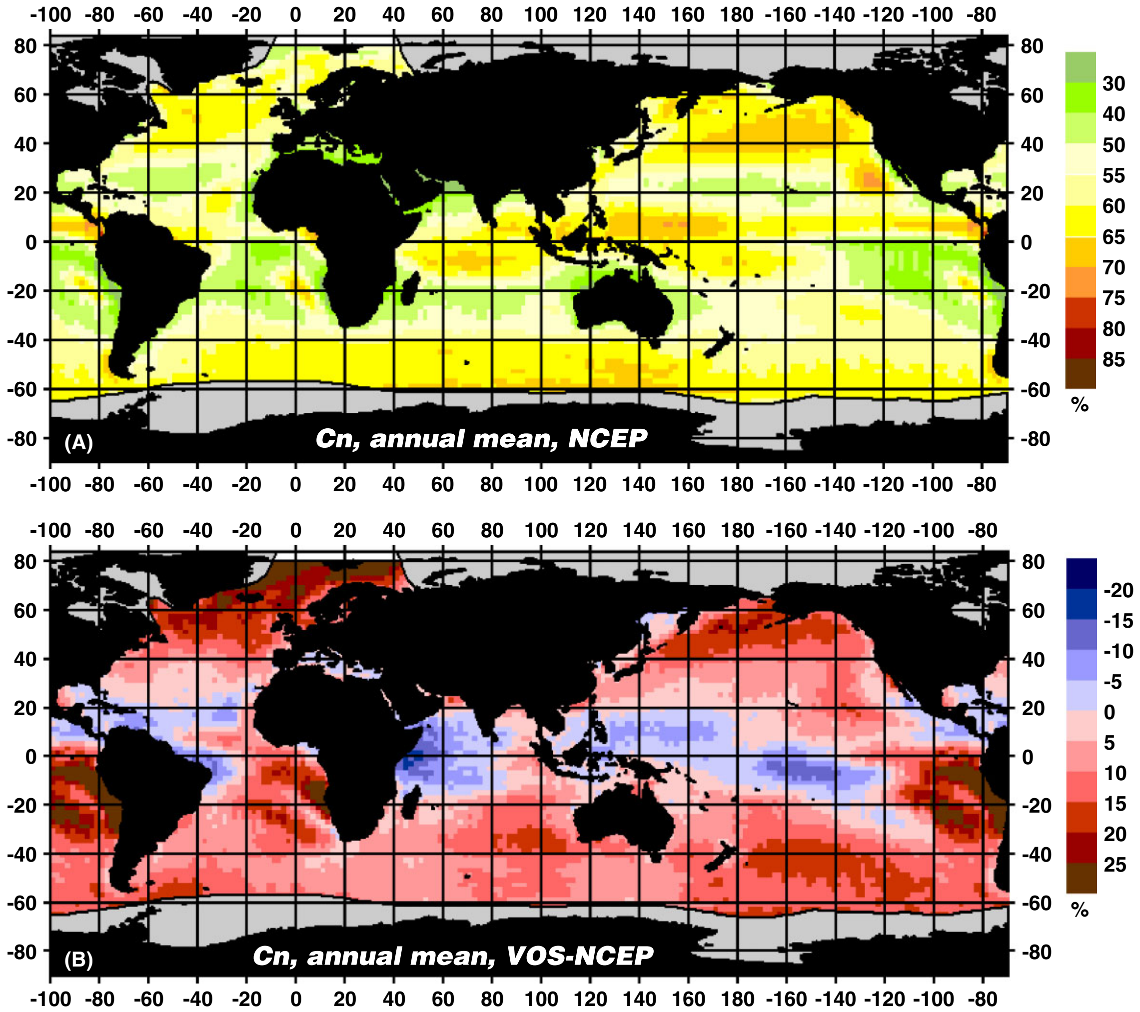

Figure 2. Climatological mean total cloud cover (%) in the NCEP-NCAR reanalysis (A) and the difference between the climatological mean total cloud cover in the VOS data and NCEP-NCAR reanalysis (B). This figure is available in colour online at www.interscience.wiley.com/ijoc

period from 1948 to 2002 (Figure 2). Figure 2(a) shows climatological distribution of the total cloud cover in the NCEP-NCAR reanalysis and Figure 2(b) displays climatological differences between the cloud amounts in the VOS and NCEP-NCAR data. In the latter, the largest values of climatological cloud cover amount to 60–70% in the midlatitudinal and equatorial regions with the smallest climatological cloud cover of 35–50% observed in the subtropics. Climatology of the total cloud cover derived from the VOS shows much higher percentages in the mid and high latitudes where the differences between the two data sets may amount to 20–25%. Alternatively, in the equatorial regions the VOS climate mean cloud cover is smaller by 5–10%.

NCEP/NCAR gives the global average total cloud cover over the global ocean of 55.23% over the whole 55-year period. This is about 20% smaller that the global estimate derived from the VOS data (66.5%). Note that our global estimate based on the VOS data is somewhat smaller than that reported by Hahn *et al*. (1995), whose value is higher than 67%. Although Hahn *et al*. (1995) analysed only the decade from 1982 to 1991, we can also explain this global difference by the exclusion of the reports with code figure '09' from the analysis and by the impact of the night observations on our global mean. We computed the VOS global cloud cover estimates exclusively from the daylight and dark observations which were distinguished on the basis of estimation of the local solar altitude and obtained about 1.2% higher global total cloud cover during night time. Thus, global NCEP-NCAR cloud cover is strongly biased with respect to the VOS estimate by approximately 10–11%. This is a general feature of the NWP cloud cover products. Particularly, Trishchenko and Li (2000) reported similar values for the NCEP-2 reanalysis. Estimation of the global cloud cover from the VOS-like sampled NCEP-NCAR data set gives the global average of 54.7% implying 1–2% underestimation of the total cloud cover. Thus, we can conclude that being potentially important for the poorly sampled regions, sampling just loosely affects the global mean. Comparison with the ISCCP products shows that ISCCP reports a considerably larger global mean cloud cover of 71.7% (Rossow and Schiffer, 1999) over the oceans. This is 3–5% larger than the estimate based on the VOS data and is considerably larger than the value derived from reanalysis. The difference

DOI: 10.1002/joc

can be partly explained by the fact that satellites detect sub-visible cirrus clouds (Minnis *et al.*, 1993) and VOS observations do not.

Comparisons for the summer and winter seasons (Figure 3) show basically the same message as the comparisons for the climatological means (Figure 2). Total cloud cover in the NCEP-NCAR is systematically smaller than that derived form the VOS data in the mid and high latitudes and slightly higher in the tropics and equatorial areas. During boreal winter (Figure 3(a), (c)) the midlatitudinal and sub-polar differences may amount to 20–25% with the tropical differences of the opposite sign being from 7 to 15%. During boreal summer, the difference between the VOS and NCEP-NCAR total cloud cover becomes larger, approaching values of 25–20% in the Northern Hemisphere sub-polar latitudes and 27% in the mid latitudes of the Southern Hemisphere. Differences of the opposite sign (NCEP-NCAR cloud cover is larger than VOS) in the tropical regions amount to 20% in July (Figure 3(b), (d)).

Figure 4 shows the mean annual cycle of the total cloud cover averaged for the Northern and the Southern Hemispheres. For the Northern Hemisphere, the differences between the VOS and NCEP-NCAR total cloud cover vary from 6–7% during winter to about 8–9% in summer. For the Southern Hemisphere, the differences are somewhat larger being 9–10% in May–June and approaching the largest values of 13–15% in August and September. For the Southern Hemisphere there is a clear indication of the phase lag between the VOS and NCEP-NCAR cloud cover, implying approximately 2 months lag of the NCEP-NCAR Hemispheric total cloud cover with respect to that derived from the VOS data. Seasonal dependence of the zonal mean cloud cover derived from NCEP-NCAR reanalysis and 'ICOADS minus NCEP/NCAR' differences, is shown in Figure 5(a), (b). The positive differences between the VOS and the NCEP-NCAR latitudinal cloud cover (Figure 5(b)) are quite persistent during the year for the latitudes south of 15°S and north of 20°N. The largest latitudinal differences of about 20% are observed for the Northern Hemisphere sub-polar latitudes. In the sub-polar latitudes of the Southern Hemisphere, there is an indication of the pronounced seasonal cycle in the values of differences. For example, they vary from 5 to 20% at 60°S. This seasonal dependence of the difference is not as pronounced in the Northern Hemisphere, where the amplitudes of the seasonal dependence of the 'VOS minus NCEP/NCAR' values in the total cloud cover amount to 5–19% at 50–60°N. Tropical zonal differences vary through the year from 0% to 5–7%, implying generally higher total cloud cover in the NCEP-NCAR in winter in the latitudinal belt from 15°S to 20°N.

Summarizing the comparison of the climatological distributions, we can point out that compared to the VOS, the NCEP/NCAR reanalysis tends to systematically

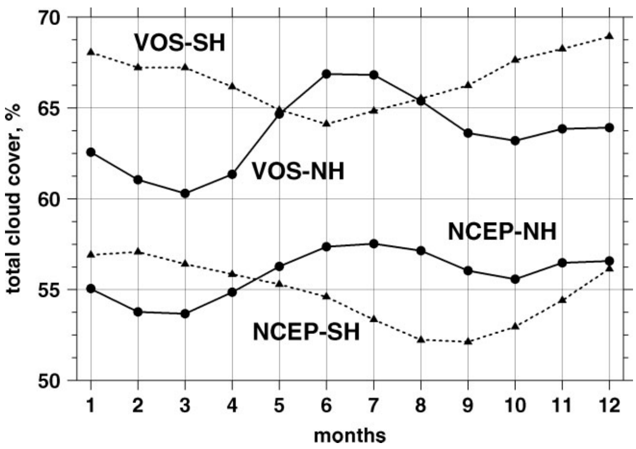

Figure 4. Seasonal March of the averaged total cloud cover (%) over the Northern Hemisphere (solid lines) and Southern Hemisphere (dashed line) from VOS (red) and NCEP-NCAR (blue) data.

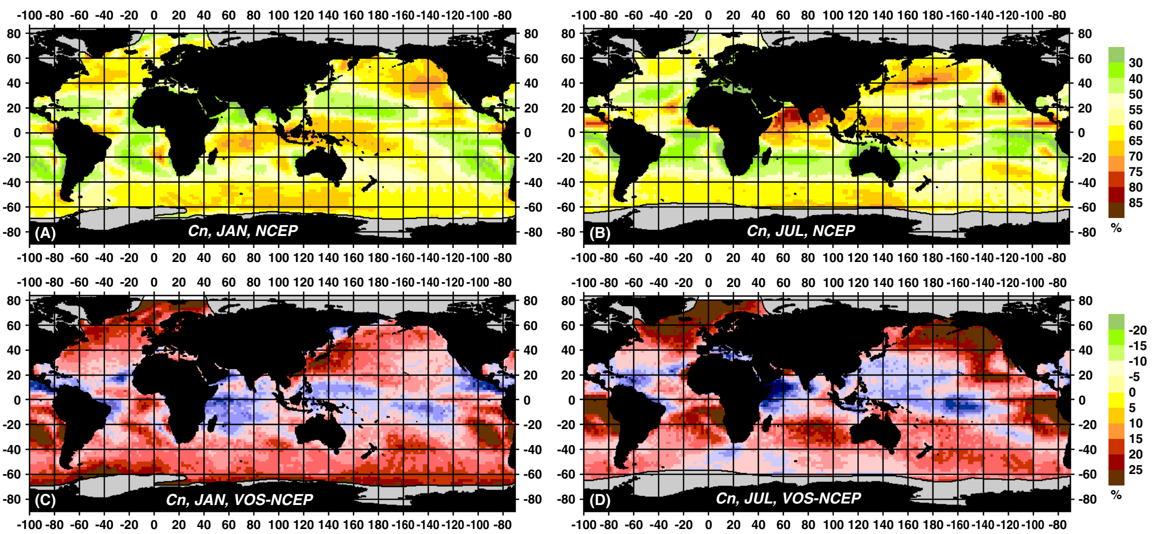

Figure 3. Climatological January (A) and July (B) total cloud cover (%) in the NCEP-NCAR reanalysis and the difference between the climatological January (C) and July (D) total cloud cover in the VOS data and NCEP-NCAR reanalysis. This figure is available in colour online at www.interscience.wiley.com/ijoc

DOI: 10.1002/joc

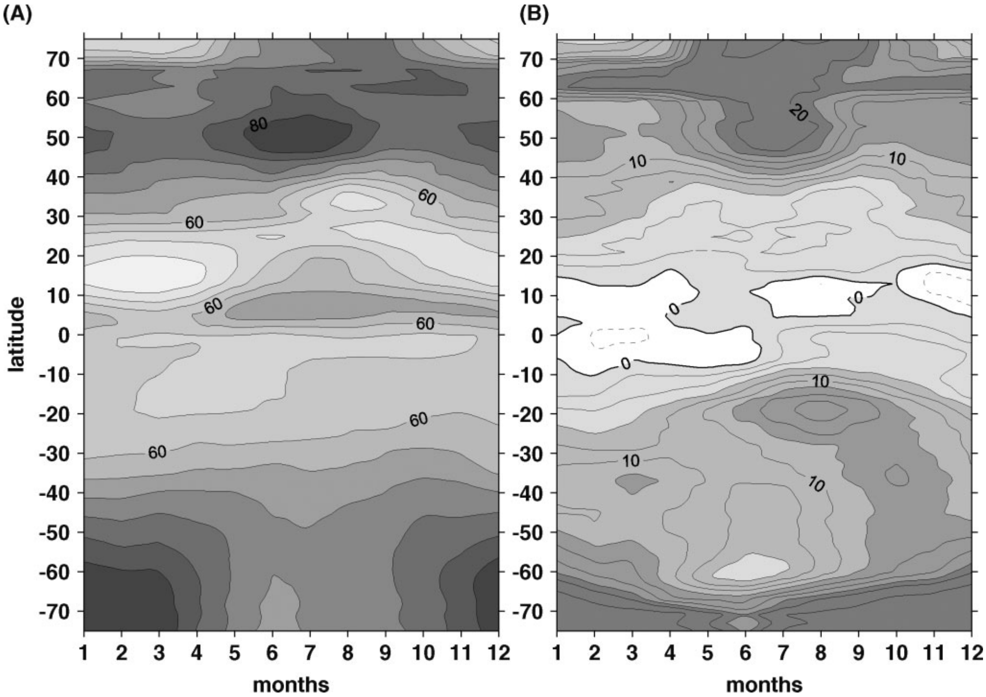

Figure 5. Seasonal March of the zonally averaged total cloud cover (%) in the NCEP-NCAR data (A) and the differences between seasonal zonally averaged total cloud covers in VOS and NCEP-NCAR (B).

underestimate the global cloud cover with the largest differences in the sub-polar and mid latitudes in both Hemispheres. Differences of the opposite sign ranging from 1–2% in summer to 5–7% in winter and implying a higher total cloud cover in the NCEP-NCAR reanalysis are observed in the tropics.

COMPARISON OF INTER-ANNUAL VARIABILITY CHARACTERITICS IN THE NCEP-NCAR AND VOS TOTAL CLOUD COVER

Standard deviations of total cloud cover and correlation analysis

We start with the comparison of the inter-annual standard deviations (STDs), computed from the anomalies around monthly means (Figure 6) from the VOS and NCEP-NCAR total cloud cover for different seasons. This analysis should show the extent to which the levels of inter-annual variability are comparable in different data sets. During both boreal winter (January–February–March period (JFM)) and summer (July–August–September period (JAS)), NCEP-NCAR shows the highest magnitudes of inter-annual variability in the tropics where STDs amount to 10–14% of the total cloud cover. The largest variability is observed in the Pacific equatorial area where the inter-annual STDs vary from 14 to 17% in boreal winter and it is somewhat smaller in boreal summer. Inter-annual STDs in mid latitudes vary form 2 to 7% and are somewhat higher in the Northern Hemisphere. Figure 6(c), (d) compares STDs of inter-annual variability in the NCEP-NCAR and VOS cloud cover. The VOS data show much stronger magnitudes of variability in the Southern Hemisphere mid and sub-polar latitudes, where the differences may amount to 10% implying nearly two to three times stronger inter-annual variations. In the Northern Hemisphere the differences are considerably smaller ranging from 1 to 5%. A comparison of the magnitudes of inter-annual variability in the NCEP-NCAR and VOS total cloud cover reflects the effect of sampling. Remarkably enough in the areas along the major ship routes, Figure 6 shows somewhat weaker inter-annual variability in the VOS data over the Northern Hemisphere. The opposite sign of differences is observed in the areas of poor sampling (sub-polar latitudes of the Northern and Southern Hemisphere Oceans), where poor sampling imply an additional uncertainty in the VOS data, and thus increasing magnitudes of inter-annual variability.

Impact of the sampling on the inter-annual variability patterns in the VOS data can be easily drawn from the correlation analysis, which was performed at every grid point of the anomalies of the total cloud cover derived from the NCEP-NCAR and VOS data for the period from 1948 to 2002. Correlation maps for the boreal winter (JFM) and boreal summer (JAS) are shown in Figure 7. For most regions of the World Ocean, they imply that inter-annual variability in the VOS cloud cover is just loosely connected with the NCEP-NCAR total cloud cover. Statistically significant correlations are observed for both seasons only in the North Atlantic and North Pacific subtropics; however, even here the correlations are typically smaller than 0.7–0.75 implying that just about 50% of the variability in one data set can be explained by the variability in the other. Figure 7(c), (d) show the correlation computed between the original NCEP-NCAR total cloud cover and that derived from the

DOI: 10.1002/joc

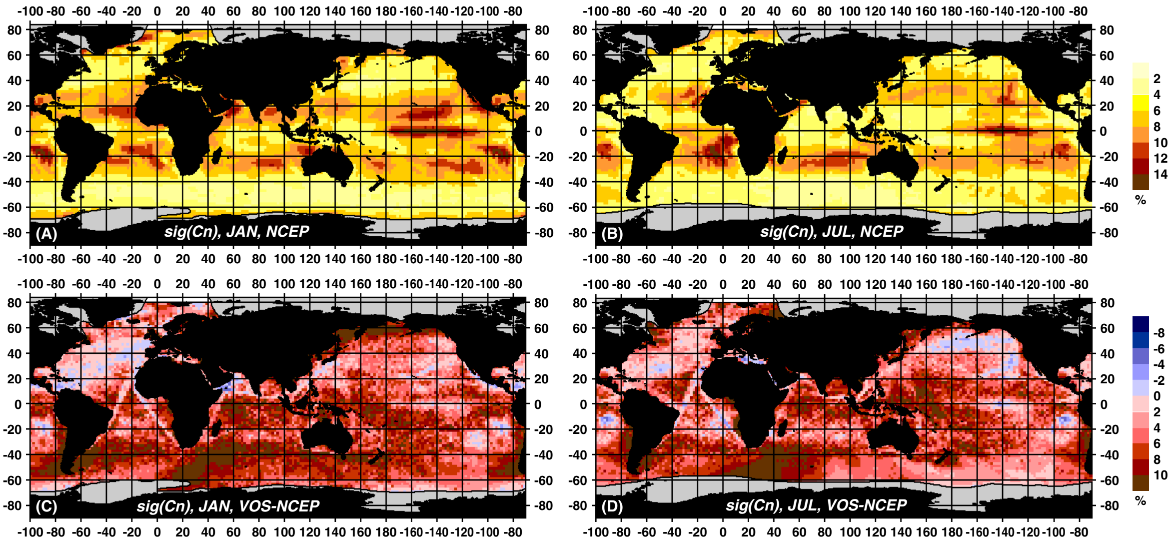

Figure 6. Inter-annual standard deviations of the total cloud cover in the NCEP-NCAR data for January (A) and July (B) and the difference between the inter-annual standard deviations derived from VOS and NCEP-NCAR data for January (C) and July (D). This figure is available in colour online at www.interscience.wiley.com/ijoc

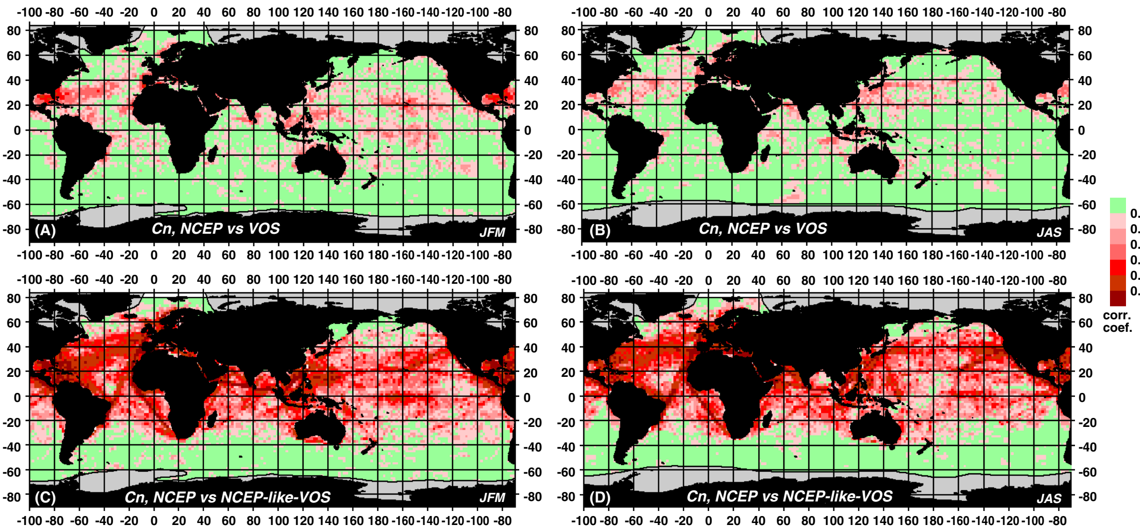

Figure 7. Correlation between the boreal winter (A), (C) and boreal summer (B), (D) anomalies of the total cloud cover from VOS and original NCEP-NCAR data (A), (B) and between the original and VOS-like sampled NCEP-NCAR data (C), (D). This figure is available in colour online at www.interscience.wiley.com/ijoc

VOS-like sampled NCEP-NCAR data set. This picture quantifies the extent to which the consistency between the two products can be affected by the sampling effect. In well sampled mid latitudes and along the major ship routes, the correlation in both seasons is typically higher than 0.8, implying close agreement between inter-annual variations. Alternatively, in poorly sampled areas, correlation drops to the values of 0.4–0.6 and to almost insignificant values everywhere in the Southern Ocean. Thus, sampling can seriously affect the inter-annual variability in the areas where observations are sparse. Nevertheless, given a very low level of correlation coefficients in Figure 7(a), (b), sampling cannot fully explain disagreements in the inter-annual variability in the VOS and NCEP-NCAR total cloud cover. In the further analysis, we will try to consider secular changes and variability associated with the major climate modes in order to put more light on this inconsistency.

Linear trends in the VOS and NCEP/NCAR total cloud cover

Secular changes in the total cloud cover are of a special interest, because the increasing cloud amount implies the decreasing diurnal range of temperatures, largely affecting the diurnal cycle on the globe (IPCC, 2001). Linear trends in NCEP-NCAR can be affected by the changes in data assimilation input. Secular changes in the VOS cloudiness may reflect temporal inhomogeneity of sampling, besides the natural signal, especially in poorly observed regions. In this respect, our trend analysis is not targeted on the quantification of climate trends. Our intention is to assess the comparability of secular changes in the two products and to estimate the role of sampling in the disagreement observed. We computed linear trends for the 55-year period from 1948 to 2002 from the NCEP/NCAR and from the ICOADS data. Figure 8 shows seasonal estimates of the linear trend at every grid point computed for both data sets together with their statistical significance, estimated according to a Student t-test. The areas where the trends are not significant at 95% are blanked in white.

VOS data show statistically significant positive trends during the 55-year period over the Atlantic tropics and midlatitudinal Pacific in both boreal winter (JFM) and boreal summer (JAS) as well as over the tropical Indian Ocean during boreal winter. These trends are ranging from 1 to 3% of the total cloud cover per decade implying 5–15% increase of the total cloud cover in these areas during the period of observations. Stronger positive trends which amount to 5% per decade are observed in the VOS data in poorly sampled sub-polar latitudes of the Pacific Ocean in summer and in the Southern Ocean during austral winter (JAS). These secular changes can be probably attributed to the temporally inhomogenous sampling. Estimates of Worley *et al*. (2005) and Gulev *et al*. (2007) show that there has been considerable increase of the number of samples between the 1950s and the 1960s and some noticeable decrease of the number of reports in 1990s with respect to the earlier period. The latter was particularly pronounced in the sub-polar North Atlantic where Figure 8(a) shows significantly negative changes in the total cloud cover of about 1–3% per decade.

The global trend pattern in the NCEP/NCAR reanalysis total cloud cover (Figure 8(c), (d)) is considerably different from that implied by the VOS. reanalysis shows secularly decreasing total cloud cover in the tropics with the magnitudes of 1–3% in boreal winter and up to 5% in boreal summer. The strongest decrease is observed in the equatorial Pacific. Tropical decrease of the total cloud cover in the Pacific can be associated with the changes in the sea surface temperature (SST), affecting the production of the convective clouds in the tropics. We can note here that massive convection can even reduce the cloud cover, when the strong local uplifting areas are balanced by large sinking areas (Sun and Lindzen, 1993). Positive trends are observed in the mid latitudes of the Southern Hemisphere Oceans where they amount to 2% per decade. Comparing the trend patterns derived from the VOS (Figure 8(a), (b)) and the NCEP-NCAR (Figure 8(c), (d)) total cloud cover data, one can find a little consistency in secular changes between the two data sets. Over the major part of the World Ocean VOS cloud cover show secular growth during the period studies. This contradicts with the trends derived from the NCEP-NCAR reanalysis, which show downward tendencies in the tropics and in western midlatitudinal Pacific. It is interesting to quantify the extent to which the disagreement observed can be explained by sampling problems in the VOS data. In order to assess the impact of sampling we computed the linear trends from the VOS-like sampled NCEP-NCAR cloud cover (Figure 8(e), (f)). The results obtained, however, do not support the assumption that different trends in total cloudiness in the NCEP-NCAR and VOS are due to exclusively sampling problem. Figure 8(e), (f) indicate that this is very likely the case for the poorly sampled areas in the Northern Hemisphere sub-polar latitudes, especially in the Pacific where trends change sign form the negative to the positive when computed form the original (regularly sampled) and VOS-like sampled NCEP-NCAR total cloud cover data. However, over most areas in the tropics and in the Southern Ocean trends show just quantitative but not qualitative differences implying that sampling cannot be responsible for the disagreement observed.

IDENTIFICATION OF THE LEADING CLIMATE MODES IN THE CLOUD FIELDS OF NCAR/NCAR AND VOS DATA

Association of the total cloud cover with the North Atlantic Oscillation

Climate variability associated with the NAO affects Europe and North America on timescales from several years to several decades (Hurrell, 1995), implying strengthening/weakening of the westerly winds and the intensity of midlatitudinal storm tracks under high/low NAO phases. Midlatitudinal cloud cover, being an essential component of the atmospheric synoptic transients, should have marked signatures of this mode in its interannual variability. In order to analyse the association of the total cloud cover with the NAO, we performed the EOF analysis of the winter (JFM) total cloud cover in the area of the Northern North Atlantic for all three analysed data sets, namely, VOS, NCEP-NCAR and VOS-like sampled NCEP-NCAR. Figure 9 shows spatial patterns corresponding to the first EOF and Figure 10(a) displays the behaviour of the first normalized principal components (PCs). First EOFs of the total cloud cover account for 34% of the total variance in the VOS data and for 28% of variance in both NCEP-NCAR based cloud products. Spatial pattern is represented by the midlatitudinal-subtropical dipole, associated with the strengthening of the midlatitudinal storm tracks under the positive NAO phase and their weakening during the negative NAO. Such a pattern is clearly evident and robust in all three data sets, showing some minor quantitative differences among them and is better visible in the NCEP-NCAR data in comparison to the ICOADS data.

The first normalized PC of this pattern for all three data sets is shown in Figure 10(a) along with the NAO index as given by Hurrell (1995). All three time series of the first normalized PCs are quite closely correlated with each other with the correlation coefficients typically higher than 0.8. This implies that the leading modes of the variability of the total cloud cover in the North Atlantic mid latitudes are quite consistent between the NCEP-NCAR and VOS data in terms of spatial pattern and the time behaviour. Correlation of the first normalized

DOI: 10.1002/joc

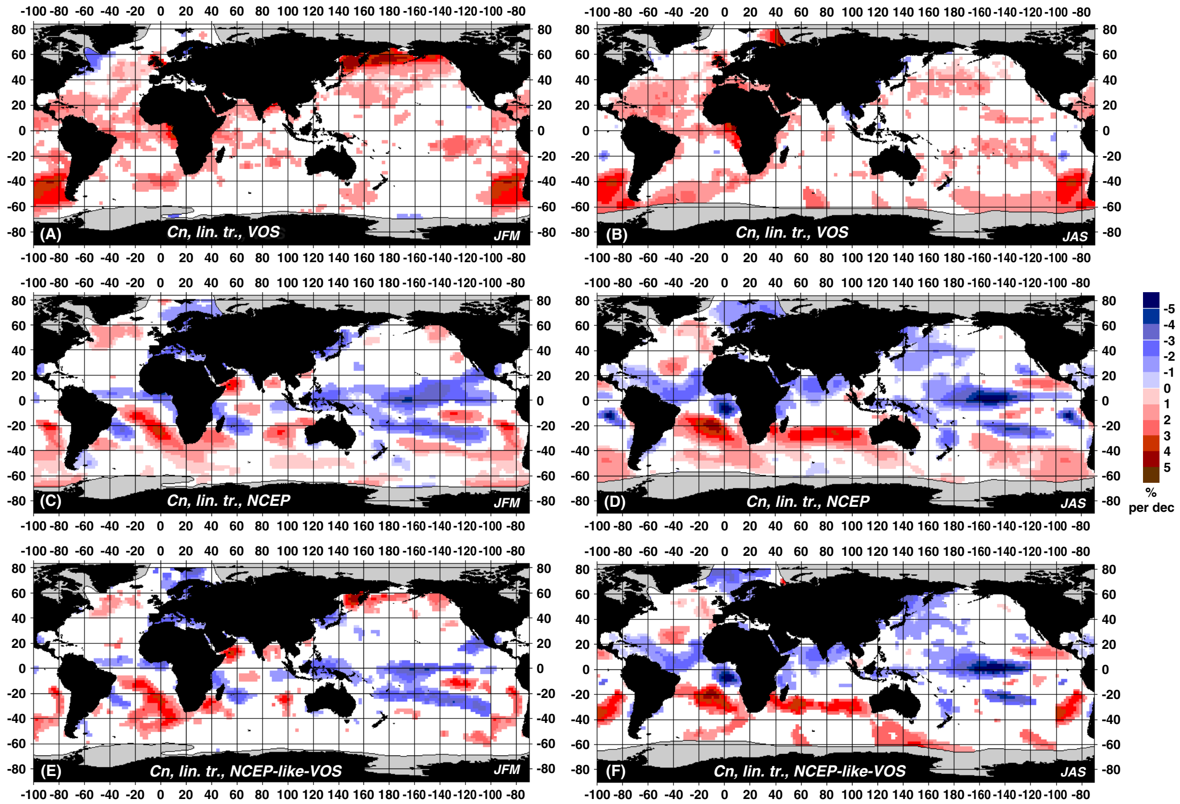

Figure 8. Linear trends (% per decade) for the winter (A), (C), (E) and summer (B), (D), (F) seasons computed from the VOS data (A), (B), original NCEP-NCAR data (C), (D) and VOS-like sampled NCEP-NCAR data (E), (F). This figure is available in colour online at www.interscience.wiley.com/ijoc

PCs with the NAO index is significant at the 95% level and varies from 0.48 for the VOS data to 0.53 for the NCEP-NCAR cloud cover. Note here that this correlation increases on longer timescale when the 3-year running mean is applied to the time series. The midlatitudinal jet stream is associated with the propagating atmospheric synoptic disturbances (cyclones) whose frontal systems are associated with different cloud types. For instance, Gulev *et al*. (2001) have shown close association of the NAO index with the number of cyclones in the midlatitudinal Atlantic. Thus, anomalies in the pressure pattern should be closely linked to the anomalies in the total cloud cover. Locally, low SLP probably provides the pre-conditioning for the upward air motions and cloud formation and vice versa. Thus, it is very natural to expect that during the high NAO phase there will be cloudier conditions than during the periods of low NAO index.

Association of the total cloud cover variability with El Niño – Southern Oscillation

ENSO represents another leading climate variability mode, which should have a clear signature in the cloud cover fields. Cloud formation in the Pacific tropics is dominated by convective and downdraft processes and should be linked to the SST variability. Increased SST in the equatorial Pacific strengthens the Hadley/Walker circulation, which leads to the increased cloudiness in the upward branch and to the reduced cloudiness in the large-scale downdrafts. Larger SST anomalies during the positive ENSO phase in the eastern tropical Pacific reduce the zonal SST gradient and thus may weaken the Walker circulation, which in turn reduces the convectively driven cloudiness above the Pacific warm pool. Detailed analysis of the mechanisms of global and regional associations between ENSO and cloudiness is provided by Park and Leovy (2004) and Wallace *et al*. (1998).

In order to assess how the ENSO mode is represented in the total cloud cover anomalies in different data sets, we computed the EOFs of the boreal winter (JFM) cloud cover in the tropical Pacific (20 °S–20°N) from the three products in the same manner as it was done for the North Atlantic. Figure 11 shows the leading EOFs which explain 22% to 25% of the total variability in the tropical Pacific cloudiness on inter-annual timescale with the largest loadings for the NCEP-NCAR data. The EOF spatial patterns are quite robust in the VOS, original NCEP-NCAR and VOS-like sampled NCEP-NCAR and are represented by the monopole pattern in the equatorial Pacific and the anomalies of the opposite sign in the eastern part of the domain. Some differences between the VOS and the NCEP-NCAR patterns corresponding to the first EOF can be identified in the Pacific tropics between 160 °E and 160 °W. Comparisons of the panels 11a and 11c show that this difference may be explained by the sampling effect, as it is clearly represented in both the VOS data and the VOS-like sampled NCEP-NCAR data and is not observed in the original NCEP-NCAR cloud product.

DOI: 10.1002/joc

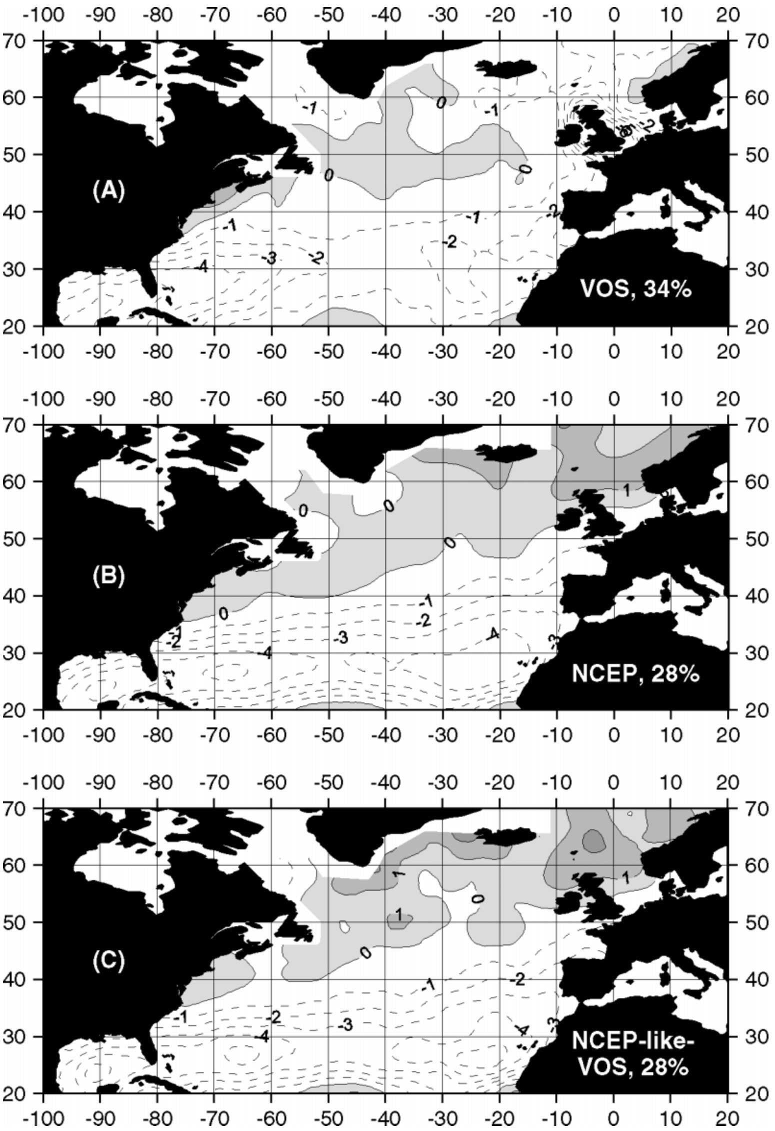

Figure 9. The first EOFs of the winter (JFM) total cloud cover anomalies derived from the VOS data (A), original NCEP-NCAR data (B) and VOS-like sampled NCEP-NCAR data (C) in the Northern North Atlantic.

Figure 10(b) shows time behaviour of the first normalized PC for the three data sets along with the Niño-3.4-index. We used the Niño-3.4-index as a measure for the SST variability in the tropical Pacific. The index was computed from SST anomalies in the Niño-3.4 region that extends from 5 °N to 5 °S and from 120 to 170 °W (Trenberth, 1997) for the period 1948–2002. The first normalized PCs of the NCEP-NCAR and the VOS-like sampled NCEP-NCAR cloud cover anomalies are highly correlated with each other with a correlation coefficient of 0.76. Correlation of both time series with the PC corresponding to the VOS data is somewhat lower (0.64). The Niño-3.4-index is highly correlated with the NCEP-NCAR PCs (correlation is higher than 0.55) and shows smaller correlation with the first PC, corresponding to the VOS cloud cover. It is interesting to note that the correlation between the NCEP-NCAR and VOS PCs and between the VOS PC and the Niño-3.4-index considerably increases for the period after the early 1970s, being quite small for the earlier decades. This can be considered as a clear indication of the sampling impact on the inter-annual variability of the cloud cover in the tropical Pacific.

SUMMARY AND CONCLUSIONS

In this study, we compared mean climatological distributions and inter-annual variability in the total cloud cover data from NCEP-NCAR and the VOS data for the last several decades. Although the pre-processing applied to the VOS data did not include some important corrections accounting for potential biases in visual observations (Hahn *et al*., 1995), our VOS-based cloud product can be considered as quite reliable on a global scale. Compared to this product, the NCEP-NCAR total cloud cover shows a strong underestimation of the total cloudiness everywhere in the mid and high latitudes by 10–25%. In the tropics, the NCEP-NCAR cloud cover is somewhat higher than that derived from the VOS data with systematic differences of 3–5%. Global and hemispheric

DOI: 10.1002/joc

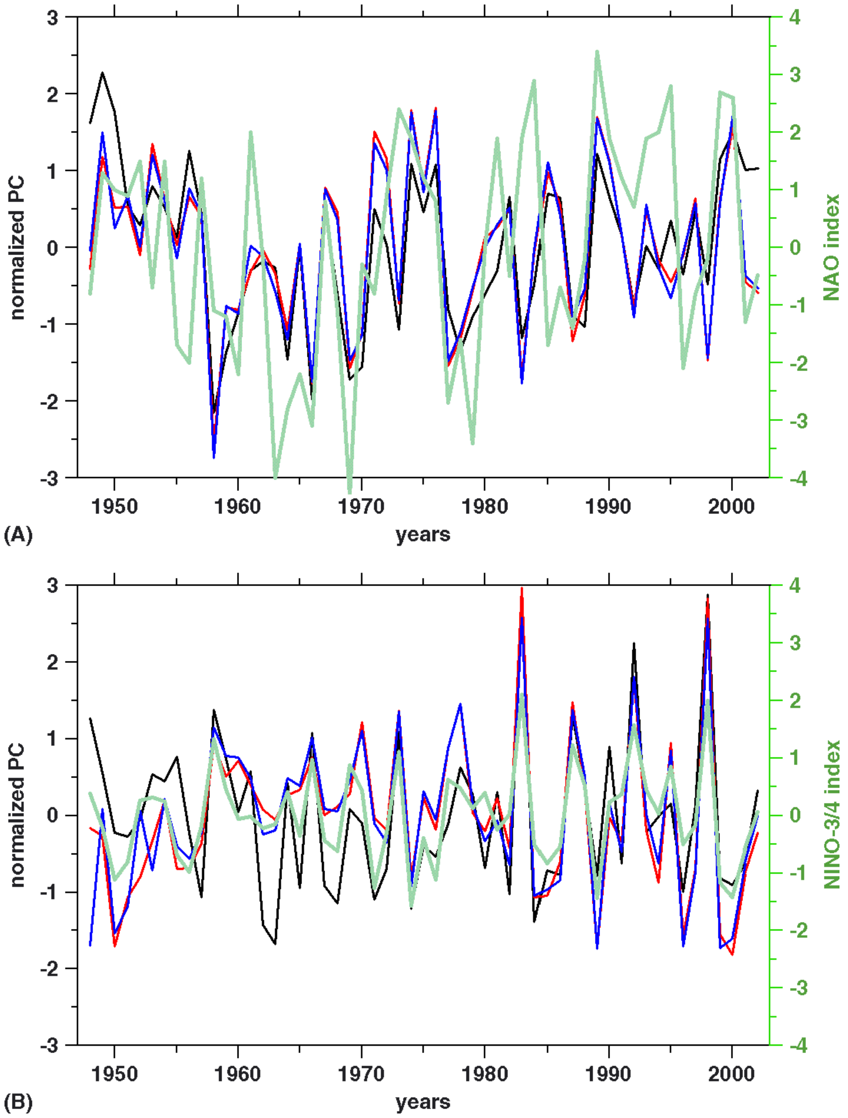

Figure 10. The first normalized PCs of the winter (JFM) total cloud cover anomalies derived from the VOS data (black), original NCEP-NCAR data (red) and VOS-like sampled NCEP-NCAR data (blue) for the North Atlantic (A) and tropical Pacific (B) along with the NAO and Nino-3,4 indices (bold green). This figure is available in colour online at www.interscience.wiley.com/ijoc

averages show typically 20% smaller total cloud cover in the NCEP-NCAR reanalysis compared to the ICOADS cloud data. Analysis of the role of sampling was performed using simulation of the actual VOS-like sampling in high-resolution NCEP-NCAR cloud cover data. It was shown that the systematic differences between the VOS and NCEP-NCAR cloud cover cannot be explained by the sampling impact in the VOS observations. This is consistent with Gulev *et al.* (2007a) who also found strong magnitudes of the random sampling errors in VOS-derived fluxes and flux-related variables, but did not report any evidence of the contribution of sampling to the biases in mean values.

Analysis of climate variability in the VOS and NCEP-NCAR total cloud cover also has shown little consistency between the two data sets for the last several decades. Strong disagreements in the strength of the variability, quantified through the inter-annual STDs and in secular changes cannot be explained by the sampling effect in the VOS data. This is different from the variability of the ocean–atmosphere fluxes analysed by Gulev *et al.* (2007b) in a similar manner. However, their analyses of variability in surface fluxes were primarily focussed on the turbulent air–sea heat exchanges with just few insights for the radiative components of the net heat flux. Despite strong disagreements obtained, we were able to identify variability patterns in the total cloud cover, which are associated with the leading modes of climate variability such as NAO and ENSO. Signatures of these modes are quite comparable in both the VOS and reanalysis cloud cover data.

Our work provides the background for further analysis of the reasons of the disagreements observed as well as for similar comparisons with alternative NWP-based cloud cover products. At this point, we can argue that climatological cloud cover is still poorly represented in the NCEP-NCAR reanalysis and probably in other reanalyses as well. Potential reason for that is

DOI: 10.1002/joc

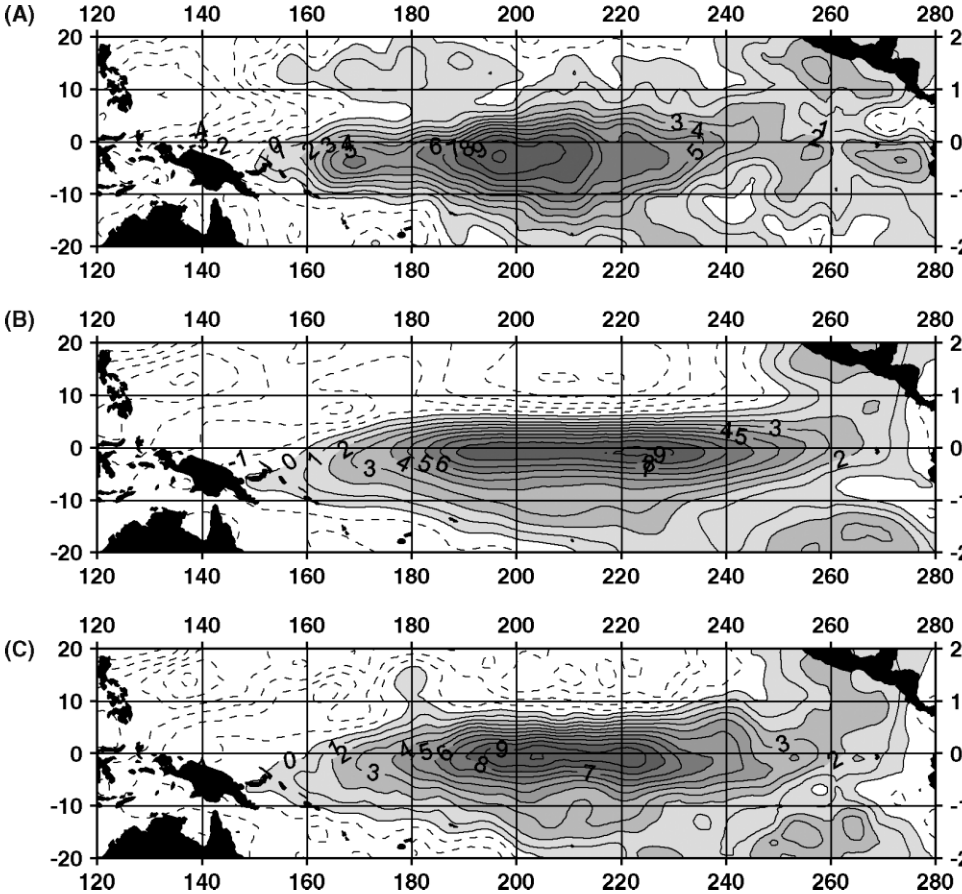

Figure 11. The first EOFs of the winter (JFM) total cloud cover anomalies derived from the VOS data (A), original NCEP-NCAR data (B) and VOS-like sampled NCEP-NCAR data (C) in the tropical Pacific.

the poor resolution of the atmospheric models used for the reanalyses. Spectral resolution of T62 of the NCEP operation model is definitely not enough for a proper representation of cloud cover properties in both tropical and midlatitudinal atmosphere. Temporal variability in the reanalyses is additionally affected by the changing data assimilation input, which may seriously affect the long-term tendencies due to assimilation of large quantity of satellite data starting from the late 1980s.

Future development of this study may go in several directions. These involve the analysis of higher resolution NWP cloud products currently available from the operational analyses of major world forecasting centres as well as from regional reanalyses produced for some limited areas already for the periods of several decades. On the other hand, further improvement should be also applied to the processing of the visual cloud data available form VOS. Guidelines of Warren *et al*. (1986, 1988) and Hahn *et al*. (1995) should be further implemented in the VOS data processing. Of a special importance is the use of satellite flux products for further quantification of biases in both VOS and NWP cloud cover data. Although short in time, these data can provide an excellent background for the global comparisons starting from the mid 1980s.

ACKNOWLEDGEMENTS

This work was supported by the Deutsche Forschungsgemeinschaft Sonderforschungsbereich SFB-460, Russian Ministry of Science and Education under the World Ocean Federal Program and by Russian Foundation for Basic Research (grant 05-05-64882). We greatly appreciate comments and suggestions of Steven Warren of University of Washington (Seattle) and anonymous reviewers, which helped to improve the manuscript. Special thanks to our colleagues Noel Keenlyside and Vladimir Semenov of IFM-GEOMAR (Kiel) for helpful comments. Considerable part of this work was done during the exchange visits of EB to Moscow and SKG to Kiel funded by AvH Stiftung (Bonn) and special grant of Russian Ministry of Science and Education.

REFERENCES

Akima EM. 1970. A new method of interpolation and smooth curve fitting based on local procedures. *Journal of Computational and Applied Mathematics* **17**: 589–602.

Chen T, Rossow WB, Zhang Y. 2000. Radiative effects of cloud-type variations. *Journal of Climate* **13**: 264–286.

da Silva AM, Young CC, Levitus S. 1994. Atlas of surface marine data 1994, vol. 2. *Anomalies of Directly Observed Quantities, NOAA Atlas NESDIS*, Vol. 7. National Oceanic and Atmospheric Administration: Silver Spring, MD; 416.

Dobson FW, Smith SD. 1988. Bulk models of solar radiation at sea. *Quarterly Journal of the Royal Meteorological Society* **114**(479): Part A: 165–182.

DOI: 10.1002/joc

Duchon CE. 1979. Lancos filtering in one and two dimensions. *Journal of Applied Meteorology* **18**: 1016–1022.

Fitzpatrick MF, Brandt RE, Warren SG. 2005. Transmission of solar radiation by clouds over snow and ice surfaces: a parameterization in terms of optical depth, solar zenith angle, and surface albedo. *Journal of Climate* **17**: 266–275.

Fowler LD, Randall DA. 1994. A global radiative-convective feedback. *Geophysical Research Letters* **21**(18): 2035–2038.

Gulev S, Zolina O, Grigoriev S. 2001. Extratropical cyclone variability in the Northern Hemisphere winter from the NCEP/NCAR reanalysis data. *Climate Dynamics* **17**: 795–809.

Gulev SK, Jung T, Ruprecht E. 2007a. Estimation of the impact of sampling errors in the VOS observations on air-sea fluxes. Part I. Uncertainties in climate means. *Journal of Climate* **20**: 279–301.

Gulev SK, Jung T, Ruprecht E. 2007b. Estimation of the impact of sampling errors in the VOS observations on air-sea fluxes. Part II. Impact on trends and interannual variability. *Journal of Climate* **20**: 302–315.

Gulev SK, Grigorieva V, Sterl A, Woolf D. 2003. Assessment of the reliability of wave observations from voluntary observing ships: Insights from the validation of a global wind wave climatology based on voluntary observing ship data. *Journal of Geophysical Research* **108**(C7): 3236, Doi:10.1029/2002JC001437.

Hahn CJ, Warren SG. 1999. *Extended edited synoptic cloud reports from ships and land stations over the Globe, 1952–1996*. Report ORNL/CDIAC-123. US Department of Energy: Publication No. 4913, 78.

Hahn CJ, Warren SG, London J. 1995. The effect of moonlight on observations of cloud cover at night, and application to cloud climatology. *Journal of Climate* **8**: 1429–1446.

Hurrell JW. 1995. Decadal trends in North Atlantic Oscillation: regional temperatures and precipitation. *Science* **269**: 676–679.

IPCC. 2001. In *Climate Change 2001 – The Science of Climate Change: Contriputions of Working Group I to the third Assesment Report of the Intergovernmental Panel on Climate Change (IPCC)*, Houghton JT, Ding J, Griggs DJ, Linden PJ, Xiaosu D (eds). Cambrige University Press: England.

Jacob C. 1999. Cloud cover in ECMWF reanalysis. *Journal of Climate* **12**: 947–959.

Josey S, Kent EK, Taylor PK. 1999. New insights into the ocean heat budget closure problem from analysis of the SOC air-sea flux climatology. *Journal of Climate* **12**: 2856–2880.

Kalnay E, Kanamitsu M, Kistler R, Collins W, Deaven D, Iredell M, Saha S, White G, Woolen J, Zhu Y, Chelliah M, Ebisuzaki W, Higgins W, Janoowiak J, Mo KC, Ropelewski C, Wang J, Leetmaa A, Reynolds R, Jenne R, Joseph D. 1996. The NCEP/NCAR 40-year reanalysis project. *Bulletin of the American Meteorological Society* **77**(3): 437–471.

Kanamitsu M, Ebisuzaki W, Woollen J, Yang S-K, Hnilo JJ, Fiorion M, Potter J. 2002. NCEP-DOE AMIP-II Reanalysis (R-2). *Bulletin of the American Meteorological Society* **83**: 1631–1643.

Kent EC, Taylor PK, Challenor P. 2000. The effect of successive correction on variability estimates for climatological data sets. *Journal of Climate* **13**: 1845–1857.

Kistler R, Kalnay E, Collins W, Saha S, White G, Woolen J, Chelliah M, Ebisuzaki W, Kanamitsu M, Kousky V, van den Dool H, Jenne R, Fiorino M. 2001. The NCEP-NCAR 50-Year reanalysis: Monthly Means CD-ROM and Documentation. *Bulletin of the American Meteorological Society* **82**(2): 247–267.

Minnis P, Heck PW, Young DF. 1993. Inference of cirrus cloud properties using satellite-observed visible and infrared radiances. 2. Verification of theoretical cirrus radiative properties. *Journal of the Atmospheric Sciences* **50**: 1305–1322.

Norris JR. 1999. On trends and possible artefacts in Global Ocean cloud cover between 1952 and 1995. *Journal of Climate* **12**: 1864–1870.

Park S, Leovy CB. 2004. Marine low-cloud anomalies associated with ENSO. *Journal of Climate* **17**: 3448–3469.

Poetzsch-Heffter C, Liu Q, Ruprecht E, Simmer C. 1995. Effect of cloud types on the earth radiation buget calculated with the ISCCP C1 dataset: methodology and initial results. *Journal of Climate* **8**: 829–843.

Reed RK. 1977. On Estimating Insolation over the Ocean. *Journal of Physical Oceanography* **7**(3): 482–485.

Rossow WB. 1978. Cloud microphysics: analysis of the clouds of Earth, Venus, Mars and Jupiter. *Icarus* **36**: 1–50.

Rossow WB, Schiffer RA. 1991. ISCCP cloud data products. *Bulletin of the American Meteorological Society* **72**(1): 2–20.

Rossow WB, Cairns B. 1995. Monitoring changes of clouds. *Climatic Change* **31**: 305–347.

Rossow WB, Schiffer RA. 1999. Advances in understanding clouds from ISCCP. *Bulletin of the American Meteorological Society* **80**(11): 2261–2287.

Rossow WB, Walker AW, Beuschel DE, Roiter MD. 1996. *International Satellite Cloud Climatology Project (ISCCP) Documentaion of New Cloud Datasets*. WMO/TD-No. 737, World Meteorological Organization, Geneva, Switzerland; 115.

Sun DZ, Lindzen RS. 1993. Distribution of tropical tropospthereic water vapor. *Journal of the Atmospheric Sciences* **50**(12): 1643–1660.

Trenberth KE. 1997. The Definition of El Niño. *Bulletin of the American Meteorological Society* **78**(12): 2771–2777.

Trishchenko AP, Li Z. 2000. Intercomparisons of global surface Albedo and SW radiation budgets from multiple satellite missions and modeling. In *Tenth ARM Science Team Meeting Proceedings*, San Antonio, TX, March 13–17, 2000. 1–12.

Uppala S, co-authors. 2006. The ERA-40 reanalysis. *Quarterly Journal of the Royal Meteorological Society* **131**: 2961–3012, Doi:10.1256/qj.04.176.

Wallace JM, Rasmusson EM, Mitchell TP, Kousky VE, Sarachik ES, von Storch H. 1998. On the structure and evolution of ENSO-related climate variability in the tropical Pacific: lessons from TOGA. *Journal of Geophysical Research* **103**: 14241–14259.

Warren G, Hahn CJ, London J, Chervin RM, Jenne RL. 1986. *Global Distribution of Total Cloud Cover and Cloud Type Amounts over Land*. The Carbon Dioxide Information Analysis Center at Oak Ridge National Laboratory: Oak Ridge, TN, 37831-6050; (865) 574–3645, TN-273+STR.

Warren G, Hahn CJ, London J, Chervin RM, Jenne RL. 1988. *Global Distribution of Total Cloud Cover and Cloud Type Amounts over the Ocean*. The Carbon Dioxide Information Analysis Center at Oak Ridge National Laboratory: Oak Ridge, TN, 37831-6050; (865) 574–3645, TN-317+STR.

WGASF. 2000. *Intercomparison and Validation of Ocean-atmosphere Energy Flux Fields*. Joint WCRP/SCOR Working Group on Air-Sea Fluxes Final Rep., WCRP-112, WMO/TD-1036, 306.

Wielicki BA, Cess RD, King MD, Randall DA, Harrison EF. 1995. Mission to planet earth: role of clouds and radiation in climate. *Bulletin of the American Meteorological Society* **76**(11): 2125–2153.

Woodruff SD, Diaz HF, Elms JD, Worley SJ, Harrison EF. 1998. COADS release 2 data and metadata enhancements for improvements of marine surface flux fields. *Physics and Chemistry of the Earth* **23**(5–6): 517–526.

Worley SJ, Woodruff SD, Reynolds RW, Lubker SJ, Lott N. 2005. ICOADS release 2.1 data and products. *International Journal of Climatology* **25**(7): 823–842.